Asian Journal of Advanced Research and Reports

3(3): 1-15, 2019; Article no.AJARR.47539

Analysis of Non-Darcy MHD Flow of a Casson Fluid over a Non-linearly Stretching Sheet with Partial Slip in a Porous Medium

Bhim Sen Kala[1*]

[1]Doon University, Dehradun, 248001, Uttarakhand, India.

Author's contribution

The sole author designed, analysed, interpreted and prepared the manuscript.

Article Information

DOI: 10.9734/AJARR/2019/v3i330090
Editor(s):
(1) Dr. Rachid Masrour, Professor, Department of Solid Physics, Faculty of Sciences, National School of Applied Sciences, University of Cadi Ayyad, Safi, Morocco.
(2) Dr. Hasan Aydogan , Associate Professor, Department of Mechanical Engineering, Selcuk University, Konya, Turkey.
Reviewers:
(1) Rajib Biswas, Bangladesh University, Bangladesh.
(2) Noor Saeed Khan, Abdul Wali Khan University, Mardan 23200, Khyber Pakhtunkhwa, Pakistan.
Complete Peer review History: http://www.sdiarticle3.com/review-history/47539

Original Research Article

Received 17 November 2018
Accepted 20 February 2019
Published 09 March 2019

ABSTRACT

In this paper, we have analysed the non-Darcy MHD flow of a Casson fluid over a nonlinearly stretching sheet in a porous medium. In the mathematical model, using similarity variables, the momentum equation is transformed to non-dimensional ordinary differential equation. And then it is solved numerically using bvp4c method, a Matlab in- built bvp4c-programm. A discussion for the effects of the parameters involved on the boundary layer thickness and the magnitude of the velocity and skin friction has been done graphically and numerically using figures and tables.

Keywords: Casson fluid; magnetic parameter; darcy parameter; velocity slip parameter; forchheimrer parameter; power index parameter.

NOMENCLATURES

x and y are cartesian coordinates[m]; u the velocity components along the x- axes[m/s]; v the velocity components along the y-axes[m/s] ;K permeability parameter[m^2]; B magnetic field; B_0 magnetic constant; C_b Forchheimer coefficient; ρ the density of the fluid [kg m^{-3}]; ν kinematic

**Corresponding author: Email: bhimskala@gmail.com;*

viscosity of the fluid [m^2 s^{-1}]; μ dynamic viscosity of the fluid [kg m^{-1} s^{-1}]'; η similarity variable; ψ stream function [m^2 s^{-1}]; f non- dimensional stream function; Vs Velocity slip parameter; S non-dimensional suction or blowing parameter; γ non- dimensional Casson fluid parameter; Fs Forchheimer constant; M non- dimensional Magnetic parameter; Kp non- dimensional Permeability parameter; n is stretching index parameter; C_f local skin-friction; Re_f Reynold number.

1. INTRODUCTION

Fluid flow over a stretching sheet has many important applications: In polymer sheet manufacturing, in chemical engineering, and in metal processing in metallurgy etc. Crane [1] first initiated the study of flow of Newtonian viscous incompressible fluid over a linearly stretching sheet. He investigated the flow of viscous incompressible fluid along a stretching plate whose velocity is proportional to the distance from the slit; such situation occurs in drawing of plastic films. The study was extended to non-Newtonian fluids by many researchers.

Rajagopal [2] studied the flow of viscous incompressible fluid on moving (stretching) surface in the boundary layer region. Siddappa et al. [3] investigated the flow of visco-elastic fluid (a non-Newtonian fluid) of 'Walters's liquid B Model' for the boundary layer flow past a stretching plate. Non –Newtonian types of flow occurs in the drawing of plastic films and artificial fibres. The moving fibre produces a boundary layer in the medium. surrounding medium of the the fibre is of technical importance; in that it governs the rate at which the fibre is cooled and this in turn affects the final properties of the yarn. Andersson [4] investigated the flow of viscoelastic fluid along a stretching sheet in the presence of transverse magnetic field. Dandapat [5] investigated the effect of transverse magnetic field on the stability of flow of viscoelastic fluid over a stretching sheet.

Fang [6] studied that variable transformation method can be used to get the solution of extended Blasius equation from original Blasius equation. Ishak et al. [7] investigated the MHD flow of viscous incompressible fluid along a moving wedge under the condition of suction and injection. Mamaloukas et al. [8] have discussed some alike nature of free-parameter method and separation of variable method and have found exact solution of equation representing flow of two-dimensional visco-elastic second grade fluid over a stretching sheet.

Bataller [9] investigated the flow in the boundary layer of the viscous incompressible fluid under two situations: One about a moving plate in a quiescent ambient fluid (Sakiadis flow) and anotherthe uniform free stream flow over a resting flat-plate (Blasius flow).

Motsa, et al. [10] investigated the MHD boundary layer flow of upper-convected Maxwell (UCM) fluid over a porous stretching surface. Nadeem et al. [11] investigated the MHD boundary layer flow of a Casson fluid over an exponentially shrinking sheet. Motsa et al. [12] had analysed the MHD flow of viscous incompressible fluid over a nonlinearly stretching sheet. Rosca [13] discussed the flow of viscous electrically conducting fluid over a shrinking surface in the presence of transverse magnetic field.

Nadeem et al. [14] investigated the MHD boundary layer flow of Williamson fluid over a stretching sheet. Mukhopadhyay [15] analysed the axis symmetric boundary layer flow of viscous incompressible fluid along a stretching cylinder in the presence of uniform magnetic field and under partial slip conditions.

Akbar et al. [16] investigate the MHD boundary layer flow of Carreau fluid over a permeable shrinking sheet. Khidir [17] used spectral homotopy perturbation method and successive linearization method to solve Falker-Skan equation (A non-linear boundary value problem).

Biswas et al. [18] studied the effects of radiation and chemical reaction on MHD unsteady heat and mass transfer of Casson fluid flow past a vertical plate. Ahmmed et al. [19] analysed the unsteady MHD free convection flow of nanofluid through an exponentially accelerated inclined plate embedded in a porous medium with variable thermal conductivity in the presence of radiation.

Biswas et al. [20] investigated the effects of Hall current and chemical reaction on MHD unsteady heat and mass transfer of Casson nanofluid flow through a vertical plate. Biswas et al. [21] studied the MHD free convection and heat transfer flow through a vertical porous plate in the presence of chemical reaction. Noor et al. [22] studied the

thin film flow of a second-grade fluid in a porous medium past a stretching sheet with heat transfer.

Noor et al. [23] studied the thermophoresis and thermal radiation with heat and mass transfer in a magnetohydrodynamic thin film second-grade fluid of variable properties past a stretching sheet. Noor et al. [24] studied the magnetohydrodynamic nanoliquid thin film sprayed on a stretching cylinder with heat transfer. Samina et al. [25] studied the flow and heat transfer in water based liquid film fluids dispensed with graphene nanoparticles.

Noor et al. [26] studied the mixed convection in gravity-driven thin film non-Newtonian nanofluids flow with gyrotactic microorganisms. Zaman et al. [27] studied the non-Newtonian nanoliquids thin film flow through a porous medium with magnetotactic microorganisms. Samina et al. [28] studied the magnetohydrodynamic second grade nanofluid flow containing nanoparticles and gyrotactic microorganisms.

Noor et al. [29] studied the bioconvection in second grade nanofluid flow containing nanoparticles and gyrotactic microorganisms. Zaman et al. [30] analysed the two dimensional boundary layer flow of a thin film fluid with variable thermo-physical properties in three dimensions space. Samina et al. [31] analysed the simulation of bioconvection in the suspension of second grade nanofluid containing nanoparticles and gyrotactic microorganisms.

Noor et al. [32] studied the slip flow of Eyring-Powell nano-liquid film containing graphene nanoparticles due to an unsteady stretching sheet with heat transfer. Noor et al. [33] investigated the Brownian motion and thermophoresis effects on MHD mixed convective thin film second-grade nanofluid flow with Hall effect and heat transfer past a stretching sheet.

Noor, et al. [34] studied the Hall current and thermophoresis effects on magnetohydrodynamic mixed convective heat and mass transfer thin film flow. Noor et al. [35] studied the entropy generation in MHD mixed convection non-Newtonian second-grade nano - liquid thin film flow through a porous medium with chemical reaction and stratification.

From the above work, we have observed that flow through non-Darcy porous medium of MHD Casson fluid is not considered. This work deals with the analysis of the non-Darcy MHD flow of a Casson fluid over a nonlinearly stretching sheet in a porous medium.

2. MATHEMATICAL MODELLING

Consider the steady two-dimensional laminar boundary-layer flow of viscous, incompressible, electrically conducting non-Newtonian Casson fluid in a saturated homogeneous non-Darcy porous medium caused by nonlinearly stretching sheet placed at the bottom of the porous medium. A Cartesian coordinate system is used. The x-axis is along the direction of the continuous stretching surface (the sheet) and y-axis is normal to the x-axis (see Fig. 1). Two equal and opposite forces are applied along the sheet so that the sheet is stretched, keeping the position of the origin unaltered. The stretching velocity varies nonlinearly with the distance from the origin. A uniform magnetic field of strength B is applied normal to the sheet.

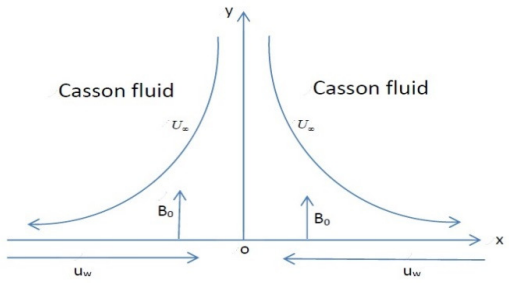

Fig. 1. Physical model and coordinate system (for stretching sheet)

We also assume that the fluid is optically dense, non-Newtonian, and without phase change. The porous medium is simulated using the well-tested and validated non-Darcian drag force model. This incorporates a linear Darcian drag for low velocity effects (bulk impedance of the porous matrix at low Reynolds numbers) and a quadratic (second order) resistance, the Forchheimer drag, for high velocity flows, as may be encountered in chemical engineering systems operating at higher velocities. Brinkman's equation takes into account the boundary effects (the viscous force).

It is assumed that the induced magnetic field, the external electric field and the electric field due to polarization of charges are negligible in comparison to the applied magnetic field. And so, all of the Hall effects and Joule heating, are neglected.

According to Nadeem et al. [11], the rheological equation for incompressible flow of Casson fluid is given by

$$\tau^{1/n} = \tau_o^{1/n} + \mu\ \dot{\gamma}^{1/n} \quad .$$

$$\tau_{ij} = 2e_{ij}\left(\mu_B + \left(p_y/\sqrt{2\pi}\right)^{1/n}\right)^n \quad .$$

Where, μ is the dynamic viscosity, μ_B is plastic dynamic viscosity of the non-Newtonian fluid, P_y is the yield stress of fluid, π is the product of the component of deformation rate with itself, namely, $\pi = e_{ij}e_{ij}$, and e_{ij} is the (i,j) th componentof the deformation rate. The value of n is greater than or equal to 1.

Under these assumptions, the governing boundary layer equations for momentum, take the following form:

The equation of continuity:

$$\frac{\partial u}{\partial x} + \frac{\partial v}{\partial y} = 0 \tag{1}$$

The Equation of Momentum:

$$u\frac{\partial u}{\partial x} + v\frac{\partial u}{\partial y} = \nu\frac{\partial^2 u}{\partial y^2} + (1+1/\gamma)\frac{\partial^2 u}{\partial y^2} - \frac{\sigma B^2}{\rho_f}u - \frac{\nu}{K}u - \frac{C_b}{\sqrt{K}}u^2 \tag{2}$$

where x and y are cartesian coordinates along the stretching sheet and normal to it respectively; u and v are the velocity components along the x- and y-axes; K is the permeability of the porous medium, B is magnetic field, C_b is Forchheimer coefficient ; ρ, ν and μ are the density, kinematic viscosity and dynamic viscosity of the fluid respectively.

To obtain similarity solution, the strength of magnetic field is assumed to vary spatially by $B(x) = B_0 x^{\frac{(n-1)}{2}}$ where B_0 is constant.

The sheet is assumed to move with power law velocity, and varies nonlinearly in spatial coordinates with some index, in the boundary layer region, so the relevant velocity boundary conditions for equations (1) to (2) are as follows:

$$\begin{aligned} &y = 0 : u = u_w(x) = c\ \mathrm{sgn}(x)|x|^n + Nv\frac{\partial u}{\partial y}, v = v_w = -V(x), -\infty < x < \infty \\ &y \to \infty : u \to 0, \end{aligned} \tag{3}$$

Where,

sgn (x) is sign of x (either it is positive or negative), c and N are constants,

$n > 0$ for accelerated sheet and $n < 0$ for decelerated sheet.

2.1 Analysis

We define

$$\begin{aligned} &\psi = \left(\frac{2\nu c}{n+1}\right)^{\frac{1}{2}} x^{\frac{n+1}{2}} f(\eta),\ \eta = \left(\frac{c(n+1)}{2\nu}\right)^{\frac{1}{2}} x^{\frac{n-1}{2}} y,. \\ &u = \frac{\partial \psi}{\partial y}, v = -\frac{\partial \psi}{\partial x}, \\ &u = cx^n f'(\eta),\ v = -\sqrt{\frac{(n+1)\ \nu\ c}{2}}\ x^{\frac{(n-1)}{2}}\left(f + \frac{(n-1)}{(n+1)}\ \eta\ f'(\eta)\right) \end{aligned} \tag{4}$$

Here,

η is similarity variable
is a stream function,

f is non- dimensional stream function, *u* is *x* -component of velocity, *v* is *y*- component of velocity.

Using equation (4), equation (2), can be written as

$$\left(\frac{1+\gamma}{\gamma}\right)f'''+ff''-\frac{2n}{n+1}(f')^2-\frac{1}{n+1}\left(\left(M+\frac{1}{\mathrm{Kp}}\right)f'+Fs(f')^2\right)=0 \tag{5}$$

And, boundary conditions (3) as

$$f(0)=S, f'(0)=1+Vs\,f''(0),\quad f'(\eta)\to 0,\ as\ \eta\to\infty. \tag{6}$$

Here prime denotes differentiation with respect to η. *Vs* is called slip parameter. $S>0$ for suction and $S<0$ for injection or blowing.

The parameters occurring in equations (5) and (6) are defined as follows:

$$M=\frac{2\sigma B_0^2}{(n+1)\rho_f c},\ \mathrm{Kp}=\frac{K c\ (n+1)x^{n-1}}{2\nu},\ Fs=\frac{2C_b\ x}{\sqrt{K}}, \tag{7}$$

γ Casson fluid parameter, Fs Forchheimer constant, M Magnetic parameter, *Kp* Permeability parameter. n is stretching index parameter.

The quantities of physical interest for this problem are the local skin-friction (C_f), and Reynold number (Re_x). These are defined as follows:

$$C_f=\frac{\tau_w}{\frac{\rho U_w^2}{2}}=\frac{\mu\left(\frac{\partial u}{\partial y}\right)_{y=0}}{\frac{\rho U_w^2}{2}}\Rightarrow C_f=\frac{2}{\sqrt{\mathrm{Re}}}\sqrt{((n+1)/2)}\ (1+1/\gamma)\ f''(0), \tag{8}$$

Where,

$\mathrm{Re}_x=U_w\ x/\upsilon$ is the local Reynold number. $\tau_w=\mu(1+1/\gamma)\left(\frac{\partial u}{\partial y}\right)_{y=0}$

3. METHOD OF NUMERICAL SOLUTION

The numerical solutions are obtained using the above equations for some values of the governing parameters, namely, the Magnetic parameter (M), the Permiability parameter (*Kp*), the Forchhemier parameter{*Fs,*), Stretching index parameter(*n*) suction or blowing parameter(S), velocity slip parameter (*Vs*) and Casson parameter(γ),. Effects of M, *Kp, Fs, n, S, Vs*, and γ, on the steady boundary layers in fluid flow region are discussed in detail. The

numerical computation is done using the Matlab in-built numerical solver bvp4c. In the computation we have taken $\eta_\infty = 15$, and axis according to the clear figure-visibility.

4. RESULTS AND ANALYSIS

For,

η_∞ =15; *M* =0;

γ = 1.00; *Kp*=inf;

Fs =0.0; *n*=0.0;

S =0.0; *Vs*=0.0;

our Matlab result for skin friction is f ''(0)= -0.443753085295389. It agrees with the results of Rosca[13] so we are confident that the present numerical method works very efficiently.

Common values of the parameters taken to draw each of the Figs. from 2 to 11:

η_∞ =15; *M* = 1; γ = 0.01; *Kp*=0.1; *Fs* =0.1; *n*=0.1; *S* =0.1; *Vs*=0.1.

Table 1. Data for values of parameters for figs. 2 to 11

	Figure 2	Figure 3	Figure 4	Figures 5,6	Figures 7,8	Figures 9,10	Figures 11
M	0.5,1,1.5	1	1	1	1	1	1
γ	0.01	0.01,0.02,0.03	0.01	0.01	0.01	0.01	0.01
Kp	0.1	0.1	0.1,0.2,0.3	0.1	0.1	0.1	0.1
Fs	0.1	0.1	0.1	0.1,0.2,0.3	0.1	0.1	0.1
n	0.1	0.1	0.1	0.1	0.1,0.2,0.3	0.1	0.1
S	0.1	0.1	0.1	0.1	0.1	0.1,0.2,0.3	0.1
Vs	0.1	0.1	0.1	0.1	0.1	0.1	0.1,0.2,0.3

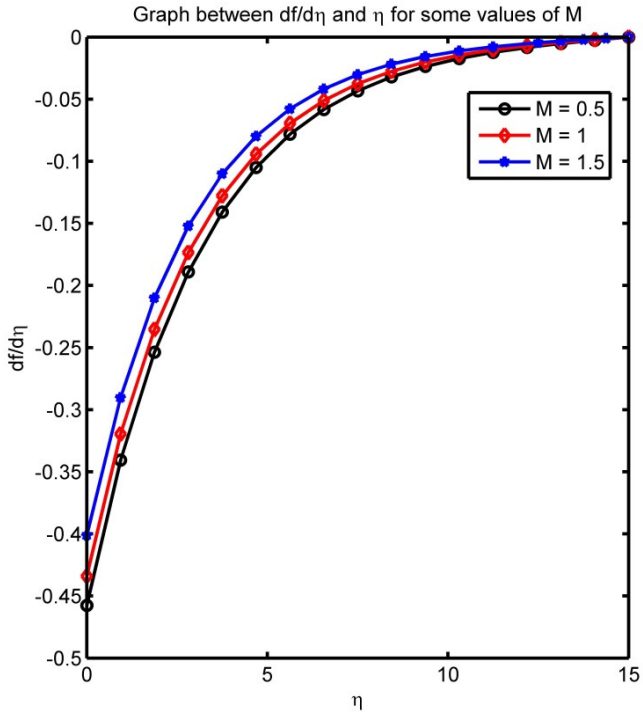

Fig. 2. Graph between $df/d\eta$ and η for different values of γ

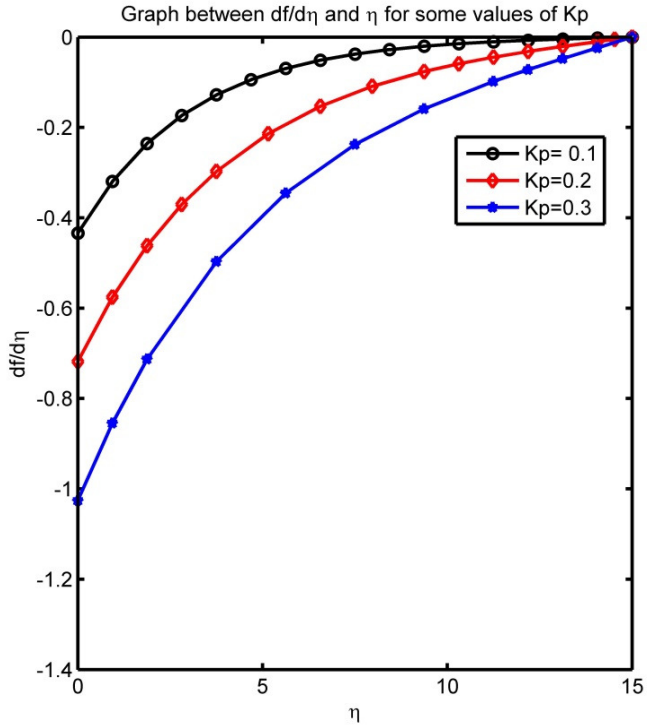

Fig. 3. Graph between $df/d\eta$ and η for different values of *Kp*

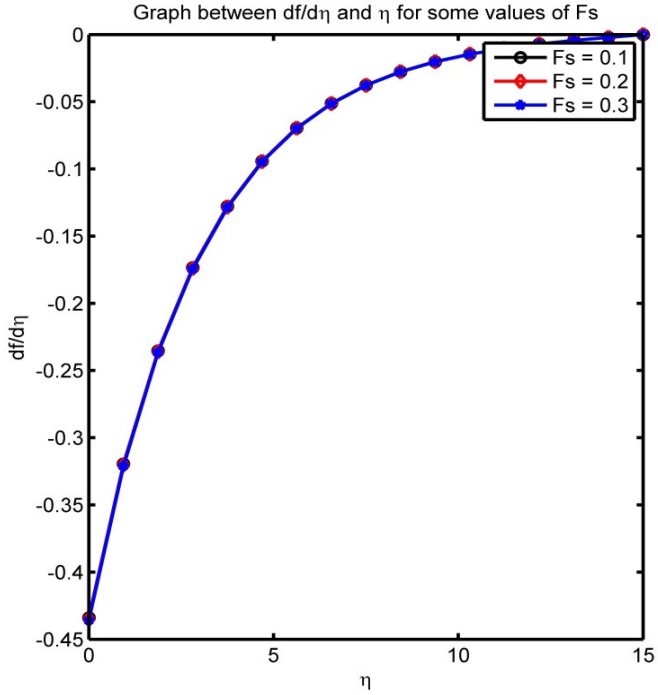

Fig. 4. Graph between $df/d\eta$ and η for different values of Fs

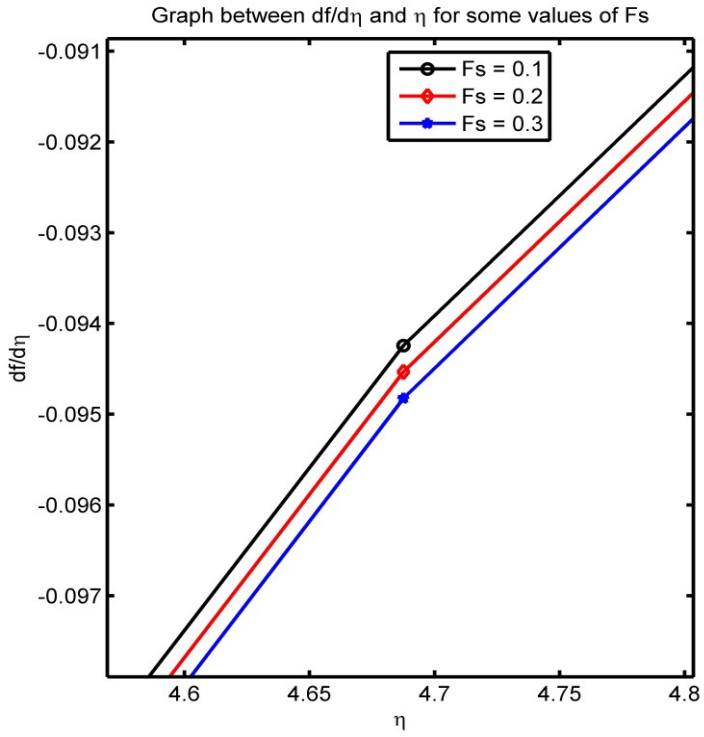

Fig. 5. Graph between $df/d\eta$ and η for different values of Fs

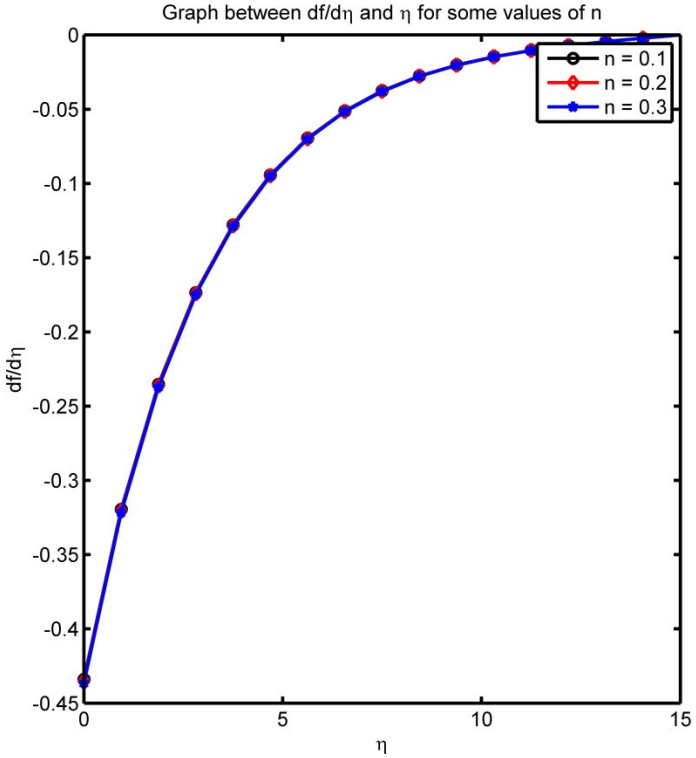

Fig. 6. Graph between $df/d\eta$ and η for different values of *n*

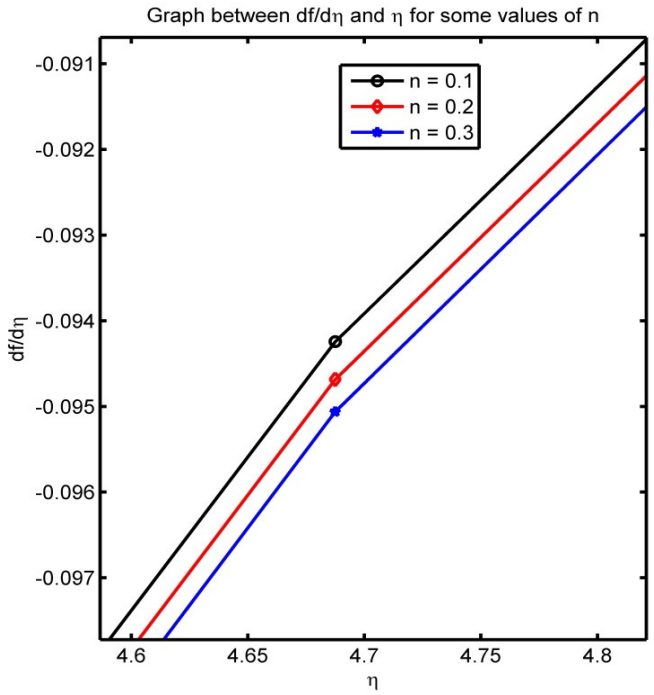

Fig. 7. Graph between $df/d\eta$ and η for different values of *n*

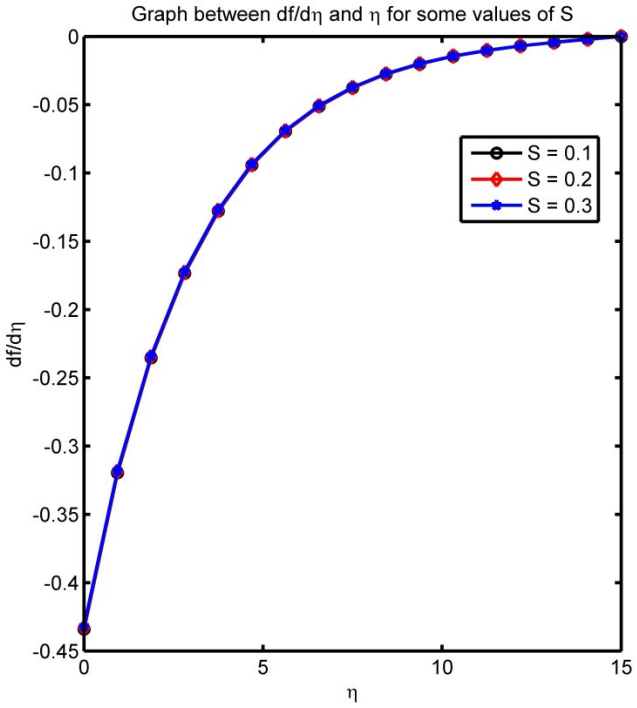

Fig. 8. Graph between $df/d\eta$ and η for different values of S

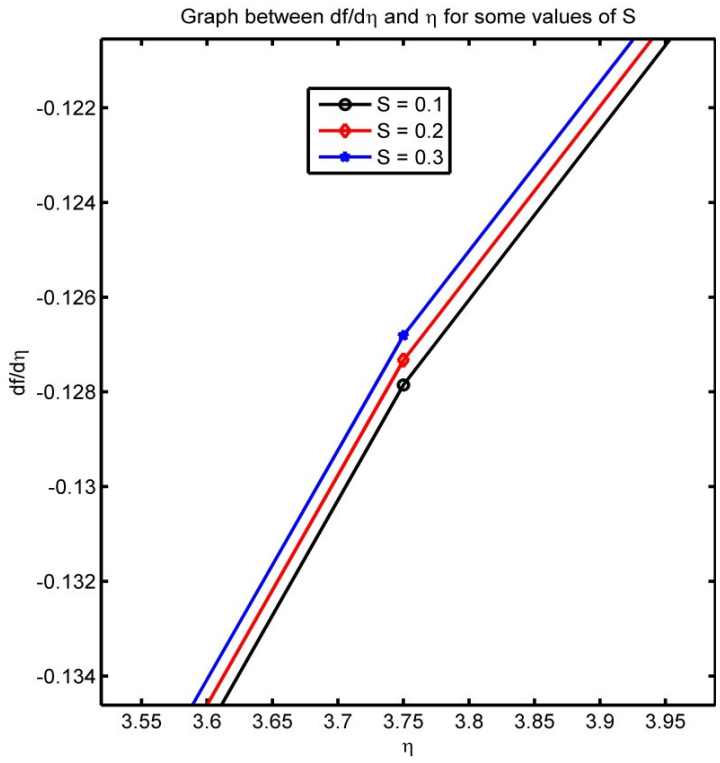

Fig. 9. Graph between $df/d\eta$ and η for different values of S

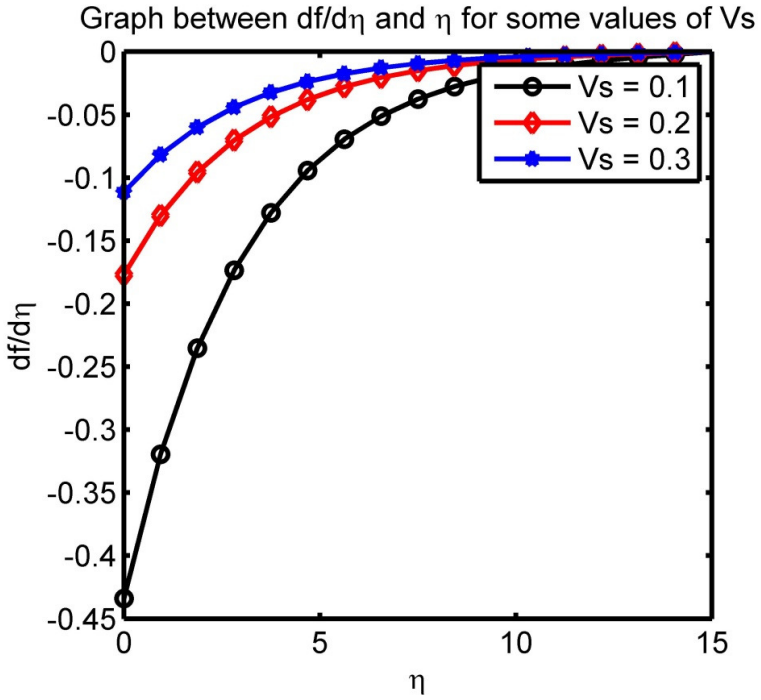

Fig. 10. Graph between $df/d\eta$ and η for different values of *Vs*

η_∞ =15; *M* = [0.5; 1.0; 1.5];

γ = [0.01; 0.02; 0.03]; *Kp*=0.1; *Fs* =0.1; *n*=0.1; *S* =0.1; *Vs*=0.1.

Table 2. Local skin friction, $f''(0)$ with respect to variation γ and M

γ	$f''(0)$ **M=0,5**	$f''(0)$ **M=1.0**	$f''(0)$ **M=1.5**
0.01	0.144315018294971	0.141980999803290	0.138732282246448
0.02	0.353659907460450	0.343383325342057	0.329639468226385
0.03	0.645481372002895	0.616151069537841	0.578963524171426

Table 2 shows for fix value of magnetic parameter, *M*, as the Casson parameter , γ , increases skin friction $f''(0)$ increases and for fix value of as the Casson parameter , γ , as magnetic parameter, *M* , increases skin friction $f''(0)$ decreases.

η_∞ =15; *M* = 1; *Kp*= [0.1; 0.2; 0.3]; *Fs* =0.1; *n*=0.1; *S* =0.1; *Vs*=0.1;

γ = [0.01; 0.02; 0.03].

Table 3. Local skin friction, $f''(0)$ with respect to variation γ and Kp

γ	$f''(0)$ **Kp=0.1**	$f''(0)$ **Kp=0.2**	$f''(0)$ **Kp=0.3**
0.01	0.141980999803290	0.170106466419974	0.200572848781858
0.02	0.343383325342057	0.506852178483415	1.615762159297962
0.03	0.616151069537841	1.776310061478046	2.738487471646433

Table 3 shows for fix value of the permeability parameter , *Kp* , as the Casson parameter, γ , increases skin friction $f''(0)$ increases and for fix value of the Casson parameter, γ , as the permeability parameter , *Kp* increases skin friction $f''(0)$ increases.

η_∞ = 15; *M* = 1; *Kp* = 0.1; *Fs* = [0.1; 0.2; 0.3]; *n*=0.1; *S* =0.1; *Vs*=0.1;

γ = [0.01; 0.02; 0.03].

Table 4. Local skin friction, $f''(0)$ with respect to variation γ and Fs

γ	$f''(0)$ **Fs=0.1**	$f''(0)$ **Fs =0.2**	$f''(0)$ **Fs =0.3**
0.01	0.141980999803290	0.142065334401625	0.142150460940992
0.02	0.343383325342057	0.344018813951724	0.344667335210914
0.03	0.616151069537841	0.618807631792279	0.621568620214765

Table 4 shows for fix value of the Forchhimer parameter, *Fs*, as the Casson parameter γ , increases skin friction $f''(0)$ increases and for fix value of the Casson parameter, γ , as the Forchhimer parameter, *Fs,* increases skin friction $f''(0)$ increases.

η_∞ = 15; *M* = 1; *Kp*=0.1; *Fs* = 0.1; *n*= [0.1; 0.2; 0.3]; *S* =0.1; *Vs*=0.1;

γ = [0.01; 0.02 ;0.03].

Table 5. Local skin friction, $f''(0)$ with respect to variation γ and m

γ	$f''(0)_{\text{n=0.1}}$	$f''(0)_{\text{n=0.2}}$	$f''(0)_{\text{n=0.3}}$
0.01	0.141980999803290	0.142109087671290	0.142218900929004
0.02	0.343383325342057	0.344351240956556	0.345194021021898
0.03	0.616151069537841	0.620216423460454	0.623849933803497

Table 5 shows for fix value of the Stretching index parameter, *n*, as the Casson parameter, γ , increases skin friction $f''(0)$ increases and for fix value of the Casson parameter, γ , as the Stretching index parameter, *n* increases skin friction $f''(0)$ increases.

η_∞ = 15; *M* = 1; *Kp* = 0.1; *Fs* = 0.1; *n* = 0.1; *S* = [0.1; 0.2; 0.3]; *Vs*=0.1;

γ = [0.01; 0.02; 0.03].

Table 6. Local skin friction, $f''(0)$ with respect to variation γ and S

γ	$f''(0)_{\text{S=0.1}}$	$f''(0)_{\text{S=0.2}}$	$f''(0)_{\text{S=0.3}}$
0.01	0.141980999803290	0.141886630792912	0.141792537905822
0.02	0.343383325342057	0.342815317844503	0.342250578490416
0.03	0.616151069537841	0.614247382976192	0.612362046919758

η_∞ = 15; *M* = 1; *Kp* = 0.1; *Fs* = 0.1; *n* = 0.1; *S* =0.1; *Vs*= [0.1; 0.2; 0.3];

γ = [0.01; 0.02; 0.03].

Table 7. Local skin friction, $f''(0)$ with respect to variation γ and Vs

γ	$f''(0)_{\text{Vs=0.1}}$	$f''(0)_{\text{Vs=0.2}}$	$f''(0)_{\text{Vs=0.3}}$
0.01	0.141980999803290	0.058268427475947	0.036674766613574
0.02	0.343383325342057	0.124416346365596	0.076086495347929
0.03	0.616151069537841	0.196471355673032	0.117245178186148

Table 6 shows for fix value of the suction or blow parameter, *S*, as the Casson parameter, γ increases skin friction $f''(0)$ increases and for fix value of the Casson parameter, γ , as the suction or blow parameter , *S* increases skin friction $f''(0)$ decreases.

Table 7 shows for fix value of the velocity slip parameter, *Vs*, as the Casson parameter, γ , increases skin friction $f''(0)$ increases and for fix value of the Casson parameter, γ , as the velocity slip parameter, *Vs* increases skin friction $f''(0)$ decreases.

4. CONCLUSION

In this paper, we have analysed the non-Darcy MHD flow of a Casson fluid over a nonlinearly stretching sheet in a porous medium. In the mathematical model, using similarity variables, the momentum equation is transformed to non-dimensional ordinary differential equation. And then it is solved numerically using bvp4c method, a Matlab in- built bvp4c-programm. A discussion for the effects of the parameters involved on the boundary layer thickness and the magnitude of the velocity and skin friction has been done graphically and numerically using figures and

tables. From this investigation, we have drawn the following conclusions:

It is seen that with the increase in the value of the magnetic parameter, *M*, the suction or blow parameter, *S*, or the velocity slip parameter, *Vs*, the boundary layer thickness and the magnitude of the velocity increases.

It is observed that with the increase in the value of the Casson parameter, γ , the permeability parameter, *Kp*, the Forchhimer parameter, *Fs*, or the Stretching index parameter, *n*, boundary layer thickness and the magnitude of the velocity decreases.

It is seen that with the increase in the value of the Casson parameter, γ , skin friction increases.

It is observed that with the increase in the value of the permeability parameter, *Kp*, or the Forchhimer parameter, *Fs*, the Stretching index parameter, *n*, skin friction increases.

It is seen that with the increase in the value of the magnetic parameter, *M*, the suction or blowing parameter, *S*, or the velocity slip parameter *Vs*, skin friction decreases.

ACKNOWLEDGEMENT

Author expresses sincere thanks to the reviewers for their time, interest and valuable comments and suggestions.

COMPETING INTERESTS

Author has declared that no competing interests exist.

REFERENCES

1. Lawrence J Crane. Flow past a stretching plate. Kurze Mitteilungen, Brief Report-Communications breves. 1970;21.
2. Rajagopal KR, Na TY, Gupta AS. Flow of viscoelastic fluid over a stretching sheet. Rheologica Acta. 1984;23:213-215.
3. Siddappa B, Abel Subhas. Non-Newtonian flow past a stretching plate. Journal of Applied Mathematics and Physics (ZAMP). 1985;36.
4. Andersson HL. Note: MHD flow of a viscoelastic fluid past a stretching surface. Acta Mechanica. 1992;95:227-230.
5. Dandapat BS, Holmedal LE, Andersson HL. Note: On the stability of MHD flow of a viscoelastic fluid past a stretching sheet. Acta Mechanica. 1998;130:143-146.
6. Fang Tiegang, Guo Fang, Lee Chia-fon F. A note on the extended Blasius equation. Applied Mathematics Letters. 2006;19: 613–617.
Available:www.elsevier.com/locate/aml,
Available:www.sciencedirect.com
7. Ishak Anuar, Nazar Roslinda, Pop Ioan. Falkner-Skan equation for flow past a moving wedge with suction or injection. J. Appl. Math. & Computing. 2007;25(1–2): 67-83
Available:http://jamc.net
8. Mamaloukas Ch, Spartalis S, Manussaridis Z. Similarity approach to the problem of second grade fluid flows over a stretching sheet. Applied Mathematical Sciences. 2007;1(7):327–338.
9. Bataller Rafael Cortell. Numerical Comparisons of Blasius and Sakiadis Flows. Matematika. 2010;26(2):187-196.
10. Motsa SS, Hayat T, Aldossary OM. MHD flow of upper-convected Maxwell fluid over porous stretching sheet using successive Taylor series linearization method. Appl. Math. Mech. -Engl. Ed. 2012;33(8):975–990.
DOI: 10.1007/s10483-012-1599-x
11. Nadeem S, Haq Rizwan Ul, Lee C. Research note: MHD flow of a Casson fluid over an exponentially shrinking sheet. Scientia Iranica B. 2012;19(6):1550–1553.
Available:www.sciencedirect.com
12. Motsa Sandile Sydney, Sibanda Precious. On the solution of MHD flow over a nonlinear stretching sheet by an efficient semi-analytical technique. International Journal for Numerical Methods in Fluids; 2012.
DOI: 10.1002/fld.2541
13. Rosca A. MHD boundary-layer flow over a permeable shrinking surface. Acta Universitatis Apulensis. 2013;36:31-38. ISSN: 1582-5329.
14. Nadeem S, Hussain ST, Lee Changhoon. Flow of a williamson fluid over a stretching sheet. Brazilian Journal of Chemical Engineering. 2013;30(03):619-625.
15. Mukhopadhyay Swati. MHD boundary layer slip flow along a stretching cylinder. Ain Shams Engineering Journal. 2013;4: 317–324.
Available:www.elsevier.com/locate/asej,www.sciencedirect.com
16. Akbar NS, Nadeem S, Haq Rizwan Ul, Ye Shiwei. MHD stagnation point flow of

Carreau fluid toward a permeable shrinking sheet: Dual solutions. Ain Shams Engineering Journal. 2014;5:1233–1239. Available:www.elsevier.com/locate/asej, Available:www.sciencedirect.com

17. Khidir Ahmed. A note on the solution of general Falkner-Skan problem by two novel semi-analytical techniques. Propulsion and Power Research. 2015; 4(4):212–220.
Available:http://ppr.buaa.edu.cn/,www.sciencedirect.com
18. Biswas R, Mondal M, Sarkar DR, Ahmmed SF. Effects of radiation and chemical reaction on MHD unsteady heat and mass transfer of Casson fluid flow past a vertical plate. Journal of Advances in Mathematics and Computer Science. 2017;23(2):1-16. Available:http://www.sciencedomain.org/issue/2795
19. Ahmmed SF, Biswas R, Afikuzzaman M. Unsteady MHD free convection flow of nanofluid through an exponentially accelerated inclined plate embedded in a porous medium with variable thermal conductivity in the presence of radiation. Journal of Nanofluids. 2018;7:891-901.
Available:http://www.aspbs.com/jon.htm.
20. Biswas Rajib, Ahmmed Sarder Firoz. Effects of Hall current and chemical reaction on MHD unsteady heat and mass transfer of Casson nanofluid flow through a vertical plate. Journal of Heat Transfer; 2018.
Available:http://asmedigitalcollection.asme.org
21. Biswasa R, Afikuzzamanb M, Mondala M, Ahmmed SF. MHD free convection and heat transfer flow through a vertical porous plate in the presence of chemical reaction. Frontiers in Heat and Mass Transfer (FHMT); 2018.
Available:www.Thermal Fluids Central.org
22. Khan Noor Saeed, Islam Saeed, Gul Taza, Khan Ilyas, Khan Waris, Ali Liaqat. Thin film flow of a second-grade fluid in a porous medium past a stretching sheet with heat transfer. Alexandria Engineering Journal; 2017.
Available:https://dx.doi.org/10.1016/j.aej.2017.01.036
23. Khan Noor Saeed, Gul Taza, Islam Saeed, Khan Waris. Thermophoresis and thermal radiation with heat and mass transfer in a magnetohydrodynamic thin film second-grade fluid of variable properties past a stretching sheet. European Physical Journal Plus. 2017;132:11.
Available:https://dx.doi.org/10.1140/epjp/i2017-11277-3.
24. Khan Noor Saeed, Gul Taza, Islam Saeed, Khan Ilyas, Alqahtani Aisha M, Alshomrani Ali Saleh. Magnetohydrodynamic nano-liquid thin film sprayed on a stretching cylinder with heat transfer. Journal of Applied Sciences. 2017;7:271.
Available:http://www.mdpi.com
25. Zuhra Samina, Khan Noor Saeed, Khan Muhammad Altaf, Islam Saeed, Khan Waris, Bonyah Ebenezer. Flow and heat transfer in water based liquid film fluids dispensed with graphene nanoparticles. Results in Physics; 2018.
Available:https://dx.doi.org/10.1016/j.rinp.2018.01.032
26. Khan Noor Saeed, Gul Taza, Khan Muhammad Altaf, Bonyah Ebenezer, Islam Saeed. Mixed convection in gravity-driven thin film non-Newtonian nanofluids flow with gyrotactic microorganisms. Results in Physics. 2017;7:4033-4049.
Available:http://dx.doi.org/10.1016/j.rinp.2017.10.017
27. Palwasha Zaman, Islam Saeed, Khan Noor Saeed, Ayaz Hamza. Non-Newtonian nanoliquids thin film flow through a porous medium with magnetotactic microorganisms. Journal of Applied Nanoscience; 2018.
Available:https://dx.doi.org/10.1007/s13204-018-0834-5
28. Zuhra Samina, Khan Noor Saeed, Islam Saeed. Magnetohydrodynamic second grade nanofluid flow containing nanoparticles and gyrotactic micro-organisms. Journal of Computational and Applied Mathematics. 2018;37:6332–6358.
29. Khan Noor Saeed. Bioconvection in second grade nanofluid flow containing nanoparticles and gyrotactic micro-organisms. Brazilian Journal of Physics. 2018;48(3):227–241, 2018;43(4):227-241.
Available:https://dx.doi.org/10.1007/s13538-018-0567-7
30. Palwasha Zaman, Khan Noor Saeed, Shah Zahir, Islamand Saeed, Bonyah Ebenezer. Study of two dimensional boundary layer flow of a thin film fluid with variable thermo-physical properties in three dimensions space. Journal of AIP Advances. 2018;8:105318.

31. Zuhra Samina Khan Noor Saeed, Shah Zahir, Islam Saeed, Bonyah Ebenezer. Simulation of bioconvection in the suspension of second grade nanofluid containing nanoparticles and gyrotactic microorganisms. Journal of AIP Advances. 2018;8:105210.
32. Khan Noor Saeed, Zuhra Samina, Shah Zahir, Bonyah Ebenezer, Khan Waris, Islam Saeed. Slip flow of Eyring-Powell nanoliquid film containing graphene nanoparticles due to an unsteady stretching sheet with heat transfer. Journal of AIP Advances. 2018;8:115302.
33. Khan Noor Saeed, Gul Taza, Islam Saeed, Khan Aurangzeb, Shah Zahir. Brownian motion and thermophoresis effects on MHD mixed convective thin film second-grade nanofluid flow with Hall effect and heat transfer past a stretching sheet. Journal of Nanofluids. 2017;6(5):812-829. Available:https://doi.org/10.1166/jon.2017.1383.
34. Khan Noor Saeed, Zuhra Samina, Shah Zahir, Bonyah Ebenezer, Khan Waris, Saeed Islam, Khan Aurangzeb. Hall current and thermophoresis effects on magnetohydrodynamic mixed convective heat and mass transfer thin film flow. Journal of Physics Communications; 2018.
Available:https://doi.org/10.1088/2399-6528/aaf830.
35. Khan Noor Saeed, Shah Zahir, Islam Saeed, Khan Ilyas, Alkanhal Tawfeeq Abdullah, Tlili Iskander. Entropy generation in MHD mixed convection non-Newtonian second-grade nanoliquid thin film flow through a porous medium with chemical reaction and stratification. Journal of Entropy. 2019;21:139.
DOI: 10.3390/e21020139

Peer-review history:
The peer review history for this paper can be accessed here:
http://www.sdiarticle3.com/review-history/47539